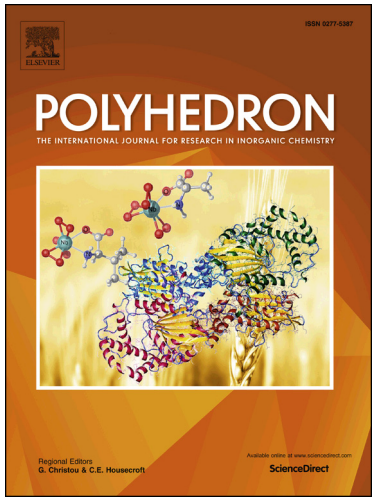

Nickel(II), zinc(II) and cadmium(II) complexes of peptides containing separate aspartyl and cysteinyl residues

Norbert Lihi, Márton Lukács, Dóra Szűcs, Katalin Várnagy, Imre Sóvágó

PII: S0277-5387(17)30400-X
DOI: http://dx.doi.org/10.1016/j.poly.2017.05.044
Reference: POLY 12663

To appear in: *Polyhedron*

Received Date: 19 April 2017
Accepted Date: 23 May 2017

Please cite this article as: N. Lihi, M. Lukács, D. Szűcs, K. Várnagy, I. Sóvágó, Nickel(II), zinc(II) and cadmium(II) complexes of peptides containing separate aspartyl and cysteinyl residues, *Polyhedron* (2017), doi: http://dx.doi.org/10.1016/j.poly.2017.05.044

Nickel(II), zinc(II) and cadmium(II) complexes of peptides containing separate aspartyl and cysteinyl residues

Norbert Lihi, Márton Lukács, Dóra Szűcs, Katalin Várnagy, Imre Sóvágó*

Department of Inorganic and Analytical Chemistry, University of Debrecen, H-4010 Debrecen, Hungary

*To whom correspondence should be addressed. E-mail: lihi.norbert@science.unideb.hu (N.L.)

Abstract

Nickel(II), zinc(II) and cadmium(II) complexes of two hexapeptides ADAAAC-NH_2 and AADAAC-NH_2 containing terminal amino, separate aspartyl carboxylate and cysteinyl thiolate donor functions have been studied by potentiometric and spectroscopic techniques. For nickel(II), the amino terminus and the aspartyl residues are the primary metal binding sites. At high pH values, thiolate groups can also coordinate to nickel(II) and this interaction results in the co-existence of various coordination isomers. In the case of AADAAC-NH_2, even dinuclear complexes can be formed with separate (NH_2,N^-,N^-,COO^-) and (S^-,$3N^-$) binding modes. On the contrary, the thiolate functions are the primary binding site for zinc(II) and especially cadmium(II) ions. The formation of macrochelate complexes is the most characteristic with these metal ions including the terminal amino, the internal carboxylate and thiolate donor functions. None of the side chain donors can, however, induce the deprotonation and zinc(II) or cadmium(II) coordination of the amide functions of these peptides.

Keywords:

nickel(II), zinc(II), cadmium(II), peptides, complexes

Synopsis

The hexapeptide AADAAC-NH_2 can form dinuclear complexes with nickel(II) ions with the (NH_2,N^-,N^-,COO^-) coordination sites from the N-terminus and (S^-,$3N^-$) binding mode from the thiolate group.

Graphical abstract

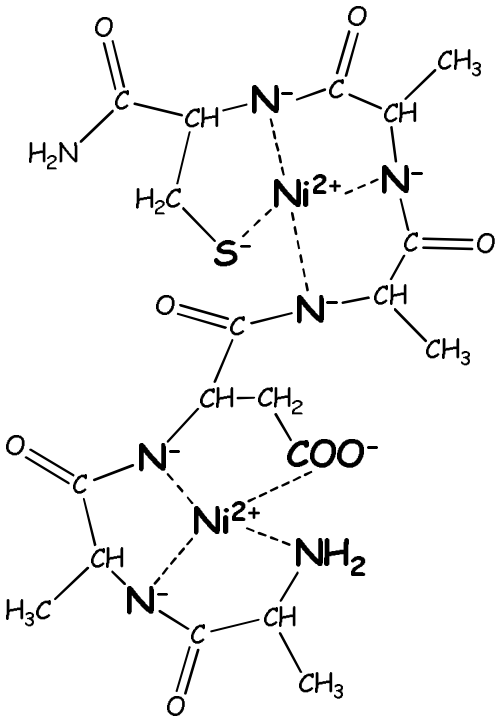

Introduction

Peptides are among the most important molecules of all living systems and take part in a great number of biochemical processes. The increasing number of publications on the metal complexes of peptides shows that the peptides are not simple organic substances but they are effective complexing agents, too. The first studies on the metal ion-peptide interactions go back to the sixties in the last century and the most important conclusions on the complexes of small model peptides are now summarized in several reviews [1-4]. The great majority of the most recent publications in metallopeptide chemistry are, however, dealing with the complex formation processes of peptide fragments of various native proteins especially those involved in neurodegeneration. These peptides are generally built up from several dozens of amino acid residues and in addition to the terminal functions they may contain a series of different donor groups in the side chains of the amino acids. These side chains can significantly influence the complex formation processes as compared to those of oligoglycines and related molecules. Moreover, the effect of side chains is very much site specific providing a great variety in the complex formation processes of large peptide molecules. It is well known that for the complexation with 3d transition metal ions the carboxylate-O of aspartyl, the imidazole-N of histidyl and thiolate-S of cysteinyl residues are the most effective donor functions. Their complex forming ability is well established if they are present as a single residue in a peptide chain and the coordination chemistry of peptides with multiple aspartyl or histidyl sites is also well clarified [5-7]. Experimental difficulties make the studies on the peptides of cysteine more complicated and only a few comprehensive studies are available in this field [8-11]. Moreover, different combinations of these functions may results in very different complex formation processes.

Systematic studies on the metal complexes of peptides containing the above-mentioned functional groups in different locations of the peptide chains may help to generalize the most important results and conclusions. In the last few years we launched a series of such systematic studies for N-terminally free but C-terminally amidated peptides containing one of the strongly coordinating groups in N-terminal position, while the other donor functions were inserted into internal or C-terminal positions. The results obtained for the complexes of hexapeptides containing Asp and His residues revealed the primary role of the amino terminus in complex formation with a significant impact from the distant histidyl residue [12]. Metal complexes of peptides containing separate histidyl and cysteinyl binding sites have also been studied and the metal ion dependence of the competition of these sites

have been demonstrated [13,14]. Complex formation with the peptides containing two cysteinyl residues in different locations have also been investigated [15]. Now in this paper we report the results obtained for the nickel(II), zinc(II) and cadmium(II) complexes of the N-terminally free hexapeptides AlaAspAlaAlaAlaCys-NH_2 (abbreviated as ADAAAC-NH_2) and AlaAlaAspAlaAlaCys-NH_2 (or AADAAC-NH_2). The interpretation of the results made it also necessary to synthesize a tetrapeptide protected at both termini, (Ac-AspAlaAlaCys-NH_2, or Ac-DAAC-NH_2) modelling the C-terminal moieties of the hexapeptides.

Experimental and computational details

Materials

Chemicals and solvents used for synthetic purposes were obtained from commercial sources in the highest available purity and used without further purification. The Rink Amide AM resin (substitution: 0.69 mmole/g), all of the N-flourenylmethoxycarbonyl (Fmoc)-protected amino acids (Fmoc-Ala-OH, Fmoc-Asp(tBu)-OH and Fmoc-Cys(Trt)-OH) and 2-(1-H-benzotriazole-1-yl)-1,1,3,3-tetramethyluronium tetrafluoroborate (TBTU) are Novabiochem (Switzerland) products. 2-methyl-2-butanol, N-hydroxybenzotriazole hydrate (HOBt·H_2O), N-methyl-pyrrolidone (NMP), 2,2'-(ethylenedioxy)diethanethiol (DODT) and triisopropylsilane (TIS) were purchased from Sigma-Aldrich Co., while N,N-diisopropyl-ethylamine (DIPEA) and trifluoroacetic acid (TFA) were Merck Millipore Co. products. Peptide-synthesis grade N,N-dimethylformamide (DMF) and acetic anhydride (Ac_2O) were bought from VWR International, while piperidine, dichloromethane (DCM), diethyl ether (Et_2O), acetic acid (AcOH) and acetonitrile (ACN) from Molar Chemicals Ltd.

The metal ion stock solution were prepared from analytical grade reagents of $NiCl_2$, $ZnCl_2$ and $Cd(NO_3)_2$ and their concentrations were checked by AAS and gravimetrically *via* the precipitation of oxinate.

Peptide synthesis and purification

In the case of the investigated peptides solid phase peptide synthesis was performed using a microwave-assisted Liberty 1 Peptide Synthesizer (CEM, Matthews, NC). Fmoc/tBtu technique and TBTU/HOBt/DIPEA activation strategy were used. Cleaving of α-amino protecting group of amino acids and resin was performed with a 20 V/V% piperidine and 0.1 M HOBt·H_2O in DMF at 80 °C with 30 W microwave power for 180 s. Four times excess of amino acids and 30 W microwave power for 300 s were used for coupling at 80 °C in the presence of 0.5 M HOBt and 0.5 M TBTU in DMF as an activator and 2 M DIPEA in NMP

as an activator base. In the case of N-terminally protected peptide (Ac-DAAC-NH_2) the free amino terminus was treated with DMF containing 5 V/V% Ac_2O and 6 V/V% DIPEA to obtain the acetylated amino group. After the finishing of synthesis, peptides were cleaved from their respective resins, with the simultaneous removal of the side chain protective groups, by treatment with a mixture of TFA/TIS/H_2O/DODT in 94/2.5/2.5/1 V/V% for 1.5 h at room temperature. Each solution containing the free peptide was separated from the resin by filtration. The crude peptides were recovered from the pertinent solution by precipitation with cold diethyl ether. The precipitate was washed and separated from it, than dried and re-dissolved in water, finally, frozen for lyophilization.

The purity of the synthesized peptides was checked by analytical RP-HPLC using a Jasco instrument equipped with a Jasco MD 2010 plus wavelength detector monitoring the absorbance at 222 nm that is characteristic for the peptide bond. The chromatographic conditions were the following: column: Europa peptide C18 (250 x 4.6 mm, 120 Å pore size, 5 µm particle size); elution: gradient elution was carried out using solvent A (0.1% TFA in water) and solvent B (0.1% in acetonitrile) at a flow rate of 1 mL·min^{-1}. From 1 min to 15 min 100% to 85% A, from 15 min to 16 min 85% A and from 16 min to 20 min 85% to 100% A was applied. The purity was also checked by ^1H NMR and mass spectrometry. Furthermore, the pH-potentiometric titrations of the ligands also confirmed the identity and purity. The schematic structures of the synthesized peptides are shown in Scheme 1.

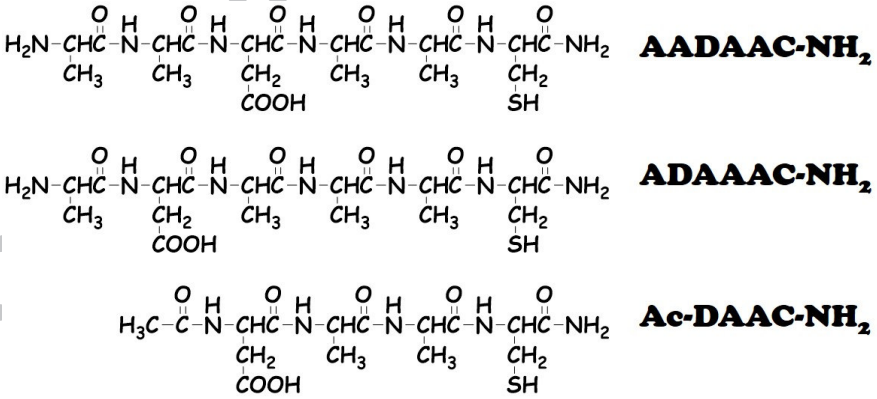

Scheme 1. Schematic structure of the synthesized peptides.

Potentiometric measurements

pH-potentiometric titrations were performed on 3.00 mL samples at 2 mM total ligand concentration with the use of carbonate free stock solution of potassium hydroxide of known concentration (~0.2 M). The metal to ligand ratios were selected between 1:2 and 2:1. During

the titrations, argon was bubbled through the samples to ensure the absence of oxygen and carbon dioxide. The samples were stirred using a VELP scientific magnetic stirrer.

All pH-potentiometric measurements were carried out at 298 K and at constant ionic strength of 0.2 M KCl in the case of nickel(II) and zinc(II) containing samples while potassium nitrate was used as a background electrolyte in the presence of cadmium(II) to avoid the formation of chlorido complexes.

pH measurements were made with a MOLSPIN pH-meter equipped with a 6.0234.110 combination glass electrode (Metrohm) and the titrant was dosed by means of a MOL-ACS burette controlled by a computer. During the titrations the following equilibrium conditions were used: the system is in equilibrium if the maximum change of pH is 0.001 unit for 30 seconds. The recorded pH readings were converted into hydrogen ion concentration as described by Irving et al [16]. Protonation constants of the ligands and overall stability ($\log\beta_{pqr}$) constants of the metal complexes were calculated by means of general computational programs (PSEQUAD [17] and SUPERQUAD [18]) based on the Eqs. (1) and (2).

$$pM + qH + rL = M_pH_qL_r \quad (1)$$

$$\beta_{pqr} = \frac{[M_pH_qL_r]}{[M]^p \cdot [H]^q \cdot [L]^r} \quad (2)$$

Spectroscopic studies

UV-visible, CD and ^{1}H NMR spectra were recorded for giving more information about the structure of the complexes formed in the investigated systems.

UV-vis spectra of the nickel(II) complexes were registered from 200 to 1100 nm on a PerkinElmer Lambda 25 scanning spectrophotometer in the same concentration range as used for pH-potentiometry. Circular dichroism spectra of nickel(II) complexes were also recorded on a Jasco J-810 spectropolarimeter using 1 mm and/or cm cells in the 220-700 nm wavelength range. Nuclear magnetic resonance (^{1}H NMR) spectra were recorded on a Bruker AM 360 MHz FT-NMR spectrometer. The chemical shifts were referenced to internal sodium 3-(trimethyl-silyl)-1-propane sulfonate (TSP, δ_{TSP} = 0 ppm) and D_2O was used as a solvent. DCl and KOD were used to set the pH of the samples. The total ligand concentration was 5 mM in the NMR experiments.

DFT methods

DFT calculations have been performed to optimize the geometry of the complexes formed in the nickel(II) containing systems and calculate the relative free energy. All calculations were performed using the Gaussian 09 (revision C.01) software package [19]. The first step was

full ground state geometry optimization using B3LYP [20] hybrid type exchange correlation functional with def2-TZVP basis set [21]. The following step was frequency calculation to determine the relative free energies of the complexes at the level of theory B3LYP/def2-TZVP. In all cases, PCM model was used to account for the effect of water [22]. The PCM model is available in Gaussian 09. Thermal contribution at 298 K with zero-point energy was also included in the calculations.

Results and discussion

Protonation macro- and micro-constants

Protonation macroconstants of the ligands have been determined by potentiometric titrations and the data are ~~involved~~ included in Table 1. In the case of ADAAAC-NH_2 and AADAAC-NH_2 three protonation constants can be determined while Ac-DAAC-NH_2 has only two protonation sites because of the lack of the terminal amino group. In agreement with previous literature studies [6,12] the lowest pK value belongs to the deprotonation of the β-carboxylic group of aspartic acid. Proton NMR measurements unambiguously prove that the first deprotonation reaction, in the pH range 3 to 5, does not affect the NMR signals of the protons of the alanyl and cysteinyl residues. On the other hand the small differences in the pK_2 and pK_3 values of ADAAAC-NH_2 and AADAAC-NH_2 strongly support that the deprotonation reactions of the thiol and ammonium functions can significantly overlap. Scheme 2 is used to demonstrate the protonation equilibria of the two hexapeptides and it is evident that the monoprotonated species $[HL]^-$ can be present in two isomeric forms denoted as (0,1,0) and (0,0,1). Evaluation of the pH-dependent NMR spectra of the two ligands made it possible to determine the protonation microconstants of the two hexapeptides [23]. The chemical shifts of the CH protons of the N-terminal Ala and CH, CH_2 protons of Cys and Asp residues were used for calculation and the microconstants are also included in Table 1 and the observed chemical shifts are available in Supplementary as Table S1. The values and the calculated speciation curves reveal that the deprotonation of the two functions significantly overlap but the ammonium group is the more acidic site in both cases. Figure S1 in the Supplement shows the speciation of the AADAAC-NH_2 peptide. In the species $[HL]^-$ of AADAAC-NH_2 the ratio of the free thiolate group is 18.3 % while this value is 23.2 % for ADAAAC-NH_2. Similar observations have already been reported for the cysteine containing dipeptides, too [24].

Table 1

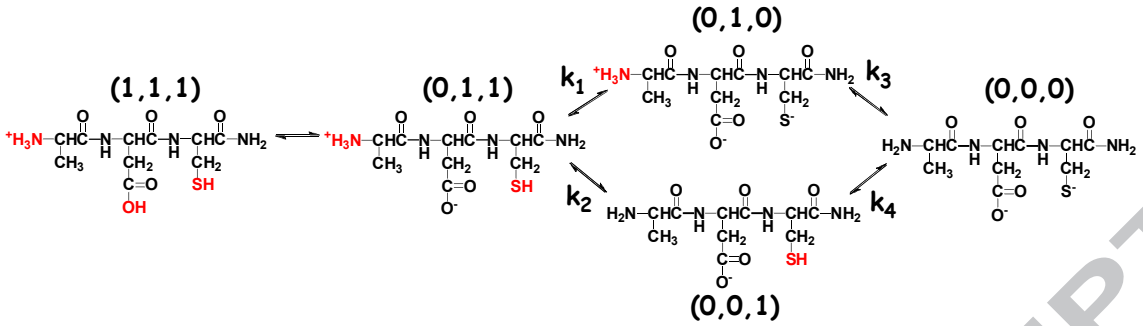

Scheme 2. Deprotonation processes of the hexapeptides. Functional groups taking part in microprocesses are marked with red color.

Nickel(II) complexes of the peptides

It has already been proved by a great number of studies that nickel(II) ions can easily form stable square planar and diamagnetic complexes with terminally free oligopeptides [1]. This process generally takes place in the pH range 7 to 10 with a cooperative deprotonation of the subsequent amide groups resulting in the formation of (NH_2,N^-,N^-,N^-) coordinated complexes. Thiolate groups can also effectively bind nickel(II) ions but the stoichiometry of the complexes largely depends on the sequence of the peptides [11]. In the presence of N-terminal cysteinyl residue the formation of (NH_2,S^-) bis(chelate) complexes results in an outstanding thermodynamic stability, similarly to the amino acids L-cysteine or D-penicillamine [25,26]. On the other hand the results reported for the peptides containing internal cysteinyl residues reveal that the thiolate group can be an effective anchor for the deprotonation and coordination of amide functions towards the N-termini [25]. Moreover, the β-carboxylate group of aspartyl residues can also have a significant contribution to the overall thermodynamic stability of metal complexes [27]. This effect is the most pronounced for the terminally free peptides containing aspartic acid as the third amino acid and was first established for the copper(II) complexes [28,29], but later studies proved that similar coordination modes are characteristic for the corresponding nickel(II) and even palladium(II) complexes, too [7, 30].

The results obtained in this study show that all the above mentioned major coordination modes can exist in the nickel(II) complexes of hexapeptides. Stability constants of nickel(II) complexes have been determined by potentiometric titrations and the values are listed in Table 2 while the speciation curves for the equimolar systems are plotted in Figure 1. The speciation of the nickel(II)-Ac-DAAC-NH_2 system is shown in Figure S2 in the supplement. The comparison of Figures 1.a and 1.b reveal that the major species formed with the two hexapeptides are the same but there are important differences in the speciation and

structure of complexes. It is also clear from the Figures 1 and S1 and Table 2 that mononuclear 1:1 complexes are formed with all three ligands while the dinuclear species are present in the nickel(II)-AADAAC-NH_2 system only. Circular dichroism and visible spectra of the nickel-AADAAC-NH_2 samples were recorded by increasing pH (see Figure 2) and these data provided evidence for the coordination modes of the major species. The absence of measurable CD extrema and the low intensity of the absorption spectra below pH 6.5 strongly support that $[NiHL]^+$ of AADAAC-NH_2 is an octahedral nickel(II) complex and thiol function is protonated in this pH range. Taking into account the microconstant of the thiol function (pk_1) log K = 12.22 - 8.53 = 3.69 can be obtained for the Ni + HL reaction. This value is close to the stability constants of the [NiL] complex of diglycine [31] (log K = 3.96) supporting the existence of (NH_2,CO) coordination mode in the species $[NiHL]^+$.

Table 2
Figure 1
Figure 2

The stochiometry of the major species is $[NiH_{-1}L]^-$ and its maximum concentration covers the physiological pH range. Both absorption and circular dichroism spectra unambiguously prove that this is a square planar nickel(II) complex. The absence of [NiL] suggests that deprotonation of two subsequent amide functions occurs upon the formation of $[NiH_{-1}L]^-$ similarly to other peptides studied previously [7] and containing aspartyl residue in the third position from the N-terminus in the peptide sequence. The comparison of the absorption and CD spectral parameters provide further support for the existence of the (NH_2,N^-,N^-,β-COO^-) coordination mode of the $[NiH_{-1}L]^-$ species. λ_{max} = 440 nm, ε = 265 $M^{-1}cm^{-1}$ were reported for absorption maxima of the same species of AspAspAsp, while its CD parameters are λ = 492 nm, Δε = –2,60 $M^{-1}cm^{-1}$ and 422 nm, +0.88 $M^{-1}cm^{-1}$. The corresponding values for the $[NiH_{-1}L]^-$ species of AADAAC-NH_2 are λ_{max} = 440 nm, ε = 278 $M^{-1}cm^{-1}$ and λ = 490 nm, Δε = –2.29 $M^{-1}cm^{-1}$ and 430 nm, +0.96 $M^{-1}cm^{-1}$. These data reveal that the coordination of the β-carboxylate function of aspartyl residue can prevent the coordination of the third amide and thiolate functions below pH 7.4. Further increase of pH is, however, accompanied with changes of absorption and CD spectra suggesting that the formation of $[NiH_{-2}L]^{2-}$ and $[NiH_{-3}L]^{3-}$ results in a significant change in the binding sites of AADAAC-NH_2. The deprotonation of the thiolate group is evident under these conditions but the involvement of a third amide group in nickel(II) binding should also occur in the $[NiH_{-3}L]^{3-}$ complex. The CD spectra of the $[NiH_{-3}L]^{3-}$ species of AADAAC-NH_2 and the model peptides tetraalanine (AAAA) and Ac-DAAC-NH_2 are shown in Figure 3 and these spectra helped to clarify the coordination

modes. It is clear from Figure 3 that CD spectrum of AADAAC-NH_2 is similar but not the same as those of AAAA and Ac-DAAC-NH_2. This observation suggests the existence of coordination isomers with (NH_2,$3N^-$) and ($3N^-$,S^-) coordination modes characteristic of AAAA and Ac-DAAC-NH_2, respectively. It is clear from Table 2 that Ac-DAAC-NH_2 easily forms the $[NiH_{-3}L]^{3-}$ species and even its stability constant is very close to that of AADAAC-NH_2. In the absence of the terminal amino group the thiolate promoted amide binding is the only possibility with Ac-DAAC-NH_2 and its characteristic positive CD extrema in basic solution can help to determine the ratio of coordination isomers. Figure 3 shows that a reasonable agreement of the calculated and measured CD spectra of AADAAC-NH_2 can be obtained if the co-existence of 25 % ($3N^-$,S^-) and 75 % (NH_2,$3N^-$) coordination modes is assumed. Thus, carboxylate function of the aspartyl residue is not a binding site in the alkaline samples but the simple oligoglycine-like coordination mode and the thiolate promoted amide binding can co-exists. The nickel(II) binding of thiolate residue is further supported by the measurements performed in the presence of excess metal ions. The data in Table 2 demonstrates that dinuclear complexes are formed only with the AADAAC-NH_2 hexapeptide with the stoichiometries $[Ni_2H_{-4}L]^-$ and $[Ni_2H_{-5}L]^{2-}$. The CD spectra of the latter complex is also shown in Figure 3 and the characteristic positive Cotton effect at 540 nm strongly supports the presence of the ($3N^-$,S^-) binding mode. The total number of the amide groups of this hexapeptide is not enough to form $[Ni_2H_{-6}L]^{3-}$ as a final species thus one of the nickel(II) ions is coordinatively unsaturated in the dinuclear species resulting in precipitation in strongly alkaline samples.

Figure 3

The comparison of Figures 1.a and 1.b reveals some important differences in the complex formation processes of ADAAAC-NH_2 and AADAAC-NH_2. In the case of nickel(II)-ADAAAC-NH_2 system the species [NiL] predominates around the physiological pH range. This stoichiometry can be obtained either by the formation of (NH_2,β-COO^-,S^-) macrochelate or by the (NH_2,N^-,β-COO^-) (5,6)-membered fused chelate with protonated thiol function. There are at least two major evidence to support the existence of the latter binding mode: (i) the results obtained for the Ac-DAAC-NH_2 and AADAAC-NH_2 unambiguously prove that thiolate binding does not occur below 7.5 – 8.0 although the same macrochelates can also be formed with AADAAC-NH_2, (ii) the very low intensity of absorption spectra and the lack of measurable CD intensity indicates the [NiL] is an octahedral complex which is characteristic of nickel(II) complexes of dipeptides with one amide nitrogen in the coordination sphere. Moreover, this explanation is in a good agreement with the stabilizing

role of aspartyl residues in position-2. A series of experimental evidence supports that β-carboxylate groups of peptides with X-Asp-Y sequences enhance the first but suppress the binding of the subsequent amide residues [7]. In accordance with this expectation the development of the intense visible absorption at λ_{max} = 422 nm and the positive and negative Cotton effects at 530 and 445 nm, respectively, starts above pH 7.5. The positive Cotton effect at 530 nm is a clear indication of the nickel(II) binding of thiolate of cysteine. Only the intensity of these absorptions increases by increasing pH supporting that the amide and thiolate deprotonation and coordination take place in overlapping processes. The final species is $[NiH_{-3}L]^{3-}$ and its CD spectra can also be obtained from the superimposition of the CD spectra of AAAA and Ac-DAAC-NH_2. The two coordination isomers are present in comparable concentrations for this ligand, 60 % and 40 % were calculated for the existence of ($3N^-$,S^-) and (NH_2,$3N^-$) coordination modes, respectively.

The major difference in the complex formation processes of the two hexapeptides is the lack of dinuclear species with ADAAAC-NH_2. Only the formation of nickel(II)-hydroxide precipitate was observed in the alkaline samples at 2:1 metal to ligand ratio. The preference of AADAAC-NH_2 for dinuclear complex formation can probably be explained by the outstanding stabilizing role of aspartyl residue in position-3 in the peptide chain.

In general, the transformation of the aspartyl residues from the third into the secondary position results in increasing nickel(II) binding ability of the C-terminal part of the peptide. In the case of AADAAC-NH_2 the distribution of the metal ion between the N- and C-terminal parts of the peptide is 75% and 25%, in contrast, this behavior was calculated as 60% and 40% for ADAAAC-NH_2. To confirm this experimental results DFT calculations were carried out and the relative free energies were calculated between the nickel(II) complexes of ADAAAC-NH_2 and AADAAC-NH_2. In all cases the geometry of both (NH_2,$3N^-$) and ($3N^-$,S^-) complexes have been optimized and to calculate the relative free energies the following equation was taking into account:

$$\Delta G_{aq}^{tot}(Ni(II):AADAAC) \rightarrow \Delta G_{aq}^{tot}(Ni(II):ADAAAC)$$

Our results indicated that the difference between ΔG_{aq}^{tot} values at 298 K is 3.9 kJ/mol if the nickel(II) is bound at the N-terminal part reflecting that ADAAAC-NH_2 is not the best binding site on the N-terminal part for the nickel(II). However, this small value of the relative free energy is not a clear-cut evidence for the preference of the nickel(II) binding to N-terminal part of the AADAAC-NH_2 peptide. From the other calculation where the C-terminal binding ability was considered ~~ΔG_{aq}^{tot} =~~ –21.7 kJ/mol was ~~obtained~~ calculated at 298 K. The

negative relative Gibbs free energy indicated that C-terminal part of ADAAAC-NH_2 is more favorable for nickel(II) than in case of AADAAC-NH_2. These values confirmed the different distribution of nickel(II) between the N- and C-terminal region of AADAAC-NH_2 and ADAAAC-NH_2. Optimized structures of the energetically preferred complexes are shown in Figure 4.

Figure 4

Zinc(II) complexes of the peptides

Stability constants of the zinc(II) complexes have been determined by potentiometric titrations and the data are summarized in Table 3, while Figure 5 shows the concentration distribution for the zinc(II)-AADAAC-NH_2 system. Mononuclear species are formed by all three ligands and there are only small differences in the speciation with the three peptides. The $[ZnHL]^+$ protonated complexes are formed in the pH range 5-7 and either ammonium or thiol groups can be protonated in these complexes. A comparison of these data with those reported for Ac-DAAC-NH_2 can help to distinguish between the two protonation sites. Protonated complexes are not formed with Ac-DAAC-NH_2 supporting a bidentate (S^-,COO^-) chelate for its [ZnL] complex. Taking into account the microscopic protonation constants of the ammonium groups (pk_2 values in Table 1) log K = 5.42 and 5.24 can be calculated for the reaction of Zn(II) + HL with AADAAC-NH_2 and ADAAAC-NH_2, respectively. These equilibrium constants are in a good agreement with the value obtained for the [ZnL] complex of Ac-DAAC-NH_2 (Table 3) supporting the same (S^-,COO^-) coordination mode. A comparison of the zinc(II) binding ability of AADAAC-NH_2 and a related hexapeptide AADAAH-NH_2 provide further support for the thiolate binding in the protonated complexes. The latter ligand contains histidine instead of cysteine but the speciation of the two systems is quite similar. Figure 6 is used to demonstrate the distribution of zinc(II) among the two peptides in equimolar samples. It is clear from Figure 6 that the complexes formed with AADAAC-NH_2 (ligand A) predominate over AADAAH-NH_2 (ligand B) due to the stabilizing role of the sulfur coordination.

Table 3

Figure 5

Figure 6

The stability constants of the [ZnL] complexes of AADAAC-NH_2 and ADAAAC-NH_2 are quite similar but significantly higher than that of Ac-DAAC-NH_2. This difference unambiguously support the tridentate binding of the hexapeptides with the involvement of the amino, carboxylate and thiolate functions. Further increase of pH results in extra base

consuming processes followed by precipitation. These observations support the hydrolytic reactions above pH 8.0 and there is no any indication for the zinc(II) induced amide deprotonations with these peptides. In the case of Ac-DAAC-NH_2 bis(ligand) complexes are also formed in overlapping reactions with the hydrolytic processes. The absence of the bis(complex) formation with the hexapeptides probably comes from the tetrahedral coordination mode of the central zinc(II) ions. The tetrahedral coordination geometry is quite common for sulfur coordinated zinc(II) complexes and the bidentate Ac-DAAC-NH_2 can easily accommodate to this geometry, while it rules out the binding of two peptides in a tridentate manner.

Cadmium(II) complexes of the peptides

Complex formation processes of zinc(II) and cadmium(II) ions are generally similar to each other but the preference for octahedral coordination geometry and the enhanced affinity for binding of thiolate residues is characteristic of cadmium(II) ions. The effects of these two major factors can be observed in this study, too. Stability constants of the cadmium(II) complexes have been determined by potentiometric titrations and the data are included in Table 4.

Table 4

Potassium nitrate was used as background electrolyte to avoid the parallel complexation with chloride ions. The corresponding speciation curves of the 1:2 samples are shown by Figure 7 for AADAAC-NH_2 and ADAAAC-NH_2, while those of Ac-DAAC-NH_2 are included in the Supplement (Figure S4).

Figure 7

It is clear from Figure 7 that cadmium(II) complexes starts to form in slightly more acidic solutions than those of the nickel(II) and zinc(II) complexes resulting in the highest stability constants for the cadmium(II) species. This is best represented by Figure 8 where the ratios of the various metal complexes formed in a model system is shown containing all three metal ions and the peptide ADAAAC-NH_2 in equimolar concentration. The predominance of cadmium(II) complexes is evident in the whole physiologically relevant pH range but binding to nickel(II) becomes the most preferred at high pH values due to the formation of amide and thiolate coordinated species. Complexation with zinc(II) overlaps with that of cadmium(II) but with a significantly lower thermodynamic stability. Moreover, complex formation with zinc(II) can compete with nickel(II) only below pH 8.0

Figure 8

Protonated complexes are formed with both hexapeptides and the equilibrium constants for the reaction Cd(II) + HL are log K = 6.41 and 6.98 for ADAAAC-NH_2 and AADAAC-NH_2, respectively. These values can be compared to that reported for the [CdL] species of Ac-DAAC-NH_2 in Table 4 providing an evidence for the same (S^-,COO^-) coordination mode in the protonated complexes of AADAAC-NH_2 and ADAAAC-NH_2 and in the [CdL] species Ac-DAAC-NH_2. The stability constants of the [CdL] complexes of the hexapeptides are, however, significantly higher than that of Ac-DAAC-NH_2 supporting the tridentate (NH_2,COO^-,S^-) coordination in these species. The major difference in the complex formation processes of zinc(II) and cadmium(II) ions is the formation of bis(ligand) complexes with all ligands involved in this study. In the presence of excess of ligand these species predominate in a wide pH range and can exist in various protonated forms. The high stability of these cadmium(II) complexes significantly suppresses the hydrolytic reactions and it occurs in the strongly alkaline samples only. Moreover, these observations unambiguously rule out the existence of cadmium(II) promoted amide deprotonation in any of the studied systems. The preference for bis(ligand) complex formation is a clear indication for the octahedral coordination geometry of all cadmium(II) complexes. The ratios of stepwise stability constants (see $lg(K_1/K_2)$ values in Table 4) provide further support for this coordination geometry and reveal that the formation of bis(ligand) complexes is especially enhanced for the protonated species with bidentate coordination mode. In addition the UV absorption of thiolate group gives possibility to follow the deprotonation and coordination of thiolate group. In the UV spectra of free ligand an intensive band appears around 230-240 nm parallel with the formation of L^{2-}. The coordination of the cadmium(II) ion results similar change in the UV-spectra, but it accompanies the formation of cadmium(II) complexes. The difference of the UV-spectra of free ligand and cadmium(II) complexes are well demonstrated by the S5 and S6 Figures (in Supplement) where the distribution curves of ADAAAC-NH_2 and Cd(II)-ADAAAC-NH_2 = 1:2 systems can be seen together with the change of absorption values at 232 nm. On the other hand the single spectra of the deprotonated form of the ligand and different cadmium(II) complexes can be calculated by means of PSEQUAD program as well. The molar absorption coefficient of L^{2-} (L = ADAAAC-NH_2, ~6400 $dm^3 \cdot mol^{-1} \cdot cm^{-1}$) is similar to those of mononuclear complexes ($[CdHL]^+$: ~5000 $dm^3 \cdot mol^{-1} \cdot cm^{-1}$, [CdL]: ~5200 $dm^3 \cdot mol^{-1} \cdot cm^{-1}$, $[CdH_{-1}L]^-$: ~5300 $dm^3 \cdot mol^{-1} \cdot cm^{-1}$), while the molar absorption coefficient of bis(ligand) complexes become doubled ($[CdH_2L_2]$: ~9000 $dm^3 \cdot mol^{-1} \cdot cm^{-1}$, $[CdHL_2]^-$: ~13000 $dm^3 \cdot mol^{-1} \cdot cm^{-1}$, $[CdL_2]^{2-}$: ~10700 $dm^3 \cdot mol^{-1} \cdot cm^{-1}$) These data reinforce the

coordination of one thiolate group in the mononuclear complexes and two thiolate groups in the bis(ligand) complexes. The calculated molar absorption coefficient of Ac-DAAC-NH_2 and Cd(II)-Ac-DAAC-NH_2 complexes are similar supporting the same coordination modes, namely, molar absorption coefficient of the fully deprotonated form of Ac-DAAC-NH_2 is ~4500 $dm^3 \cdot mol^{-1} \cdot cm^{-1}$, while this value is ~4000 $dm^3 \cdot mol^{-1} \cdot cm^{-1}$ and ~4500 $dm^3 \cdot mol^{-1} \cdot cm^{-1}$ in the case of [CdL] and $[CdH_{-1}L]^-$ monocomplexes, respectively. Molar absorption coefficient of the bis(ligand) complex is ~10 000 $dm^3 \cdot mol^{-1} \cdot cm^{-1}$ reflecting the presence of two thiolate groups in the coordination sphere.

Conclusions

The metal binding affinities of two hexapeptides ADAAAC-NH_2 and AADAAC-NH_2 containing terminal amino, internal aspartyl carboxylate and C-terminal cysteinyl thiolate donor functions as possible metal binding sites have been studied. The major species formed with the two hexapeptides are the same for all three metal ions but there are important differences in the speciation and structure of complexes. Moreover, the results reveal a significant difference in the affinity of the various sites to nickel(II) ions on one side and zinc(II) and cadmium(II) on the other. For nickel(II), the amino terminus is the primary ligating site and aspartyl residue in position-3 in the sequence can especially enhance the thermodynamic stability of nickel(II) complexes with (NH_2,N^-,N^-,COO^-) coordination mode. However, thiolate groups of both peptides can also coordinate to nickel(II) in the slightly alkaline samples and it results in the presence of various coordination isomers. For AADAAC-NH_2 the formation of dinuclear complexes was also suggested with the above mentioned coordination sites from the N-terminus and (S^-,$3N^-$) binding mode from the thiolate group. On the contrary, the thiolate functions are the primary binding site for zinc(II) and especially cadmium(II) ions. The formation of macrochelate complexes is the most characteristic with these metal ions including all possible donor sites. None of the side chain donor functions can, however, induce the deprotonation and zinc(II) or cadmium(II) coordination of the amide functions of these peptides. The co-existence of these different coordination modes provides a high metal ion selectivity in the complex formation processes of ADAAAC-NH_2 and AADAAC-NH_2 as it was demonstrated by Figure 8. Binding to cadmium(II) is highly favoured in the slightly acidic and neutral pH ranges. Complexation with cadmium(II) and zinc(II) is partly overlapped, but the latter species have significantly lower thermodynamic stability. The preference of nickel(II) coordination is connected to the

involvement of both amide nitrogen and thiolate sulfur atoms in metal binding but these species can be formed at high pH values only.

Acknowledgement

The research was supported by the EU and co-financed by the European Regional Development Fund under the project GINOP-2.3.2-15-2016-00008, the Hungarian Scientific Research Fund (K115480) and the Richter Gedeon Talentum Foundation. The authors thank the National Information Infrastructure Development Institute (NIIF) for awarding access to resource based in Hungary at Debrecen.

References

1. H. Sigel, R.B. Martin, Chem. Rev., 82 (1982) 385-426.
2. I. Sóvágó, K. Ősz, Dalton Trans., (2006) 3841-3854.
3. H. Kozlowski, W. Bal, M. Dyba, T. Kowalik-Jankowska, Coord. Chem. Rev., 184 (1999) 319-346.
4. I. Sóvágó, C. Kállay, K. Várnagy, Coord. Chem. Rev., 256 (2012) 2225-2233.
5. I. Sóvágó, K. Várnagy, N. Lihi, Á. Grenács, Coord. Chem. Rev., 327-328 (2016) 43-54.
6. C. Kállay, K. Várnagy, G. Micera, D. Sanna, I. Sóvágó, J. Inorg. Biochem., 99 (2005) 1514-1525.
7. C. Kállay, I. Sóvágó, K. Várnagy, Polyhedron, 26 (2007) 811-817.
8. R. Vogler, M. Gelinsky, L.F. Guo, H. Vahrenkamp, Inorg. Chim. Acta, 339 (2002) 1-8.
9. K. Krzywoszynska, M. Rowinska-Zyrek, D. Witkowska, S. Potocki, M. Luczkowski, H. Kozlowski, Dalton Trans., 40 (2011) 10434-10439.
10. M. Rowinska-Zyrek, D. Witkowska, S. Bielinska, W. Kamysz, H. Kozlowski, 40 (2011) 5604-5610.
11. D. Witkowska, M. Rowinska-Zyrek, G. Valensin, H. Kozlowski, Coord. Chem. Rev., 256 (2012)133-148.
12. M. Raics, D. Sanna, I. Sóvágó, C. Kállay, Inorg. Chim. Acta, 426 (2015) 99-106.
13. M. Raics, N. Lihi, A. Laskai, C. Kállay, K. Várnagy, I. Sóvágó, New J. Chem., 40 (2016) 5420-5427.
14. N. Lihi, D. Sanna, I. Bányai, K. Várnagy, I. Sóvágó, New J. Chem., 41 (2017) 1372-1379.
15. N. Lihi, Á. Grenács, S. Timári, I. Turi, K. Várnagy, I. Sóvágó, New. J. Chem., 39 (2015) 8364-8372.
16. H. Irving, G. Miles, L. D. Pettit, Anal. Chim. Acta., 38 (1967) 475-488.
17. L. Zékány, I. Nagypál, in: Computational Methods for the Determination of Stability Constants, ed. D. Leggett, Plenum Press, New York (1985) 291-299.

18. P. Gans, A. Sabatini, A. Vacca, J. Chem. Soc., Dalton Trans., (1985) 1195-1200.
19. M. J. Frisch, G. W. Trucks, G. E. S. H. B. Schlegel, M. A. Robb, J. R. Cheeseman, G. Scalmani, V. Barone, B. Mennucci, G. A. Petersson, H. Nakatsuji, M. Caricato, X. Li, H. P. Hratchian, A. F. Izmaylov, J. Bloino, G. Zheng, J. L. Sonnenberg, M. Hada, M. Ehara, K. Toyota, R. Fukuda, J. Hasegawa, M. Ishida, T. Nakajima, Y. Honda, O. Kitao, H. Nakai, T. Vreven, J. A. Montgomery, Jr., J. E. Peralta, F. Ogliaro, M. Bearpark, J. J. Heyd, E. Brothers, K. N. Kudin, V. N. Staroverov, R. Kobayashi, J. Normand, K. Raghavachari, A. Rendell, J. C. Burant, S. S. Iyengar, J. Tomasi, M. Cossi, N. Rega, J. M. Millam, M. Klene, J. E. Knox, J. B. Cross, V. Bakken, C. Adamo, J. Jaramillo, R. Gomperts, R. E. Stratmann, O. Yazyev, A. J. Austin, R. Cammi, C. Pomelli, J. W. Ochterski, R. L. Martin, K. Morokuma, V. G. Zakrzewski, G. A. Voth, P. Salvador, J. J. Dannenberg, S. Dapprich, A. D. Daniels, Ö. Farkas, J. B. Foresman, J. V. Ortiz, J. Cioslowski, D. J. Fox, Gaussian 09, Gaussian Inc., Wallingford CT, 2009.
20. A. D. Becke, J. Chem. Phys., 98 (1993) 5648–5652.
21. F. Weigend, R. Ahlrichs, Phys. Chem. Chem. Phys., 7 (2005) 3297-3305.
22. V. Barone, M. Cossi, J. Tomasi, J. Chem. Phys., 107 (1997) 3210.
23. K. Ősz, G. Lente, C. Kállay, J. Phys. Chem. B, 109 (2005) 1039-1047.
24. I. Sóvágó, T. Kiss, K. Várnagy, B. Decock-Le Reverend, Polyhedron, 7 (1988) 1089-1093.
25. I. Sóvágó, A. Gergely, B. Harman, T. Kiss, J. Inorg. Nucl. Chem., 41 (1979) 1629-1633.
26. H. Kozlowski, B. Decock-Le Reverend, D. Ficheux, C. Loucheux, I. Sóvágó, J. Inorg. Biochem., 29 (1987) 187-197.
27. W.J. Puspita, A. Odani, O. Yamauchi, J. Inorg. Biochem., 73 (1999) 203-213.
28. I. Sóvágó, T. Kiss, A. Gergely, Inorg. Chim. Acta, 93 (1984) L53-L55.
29. B. Decock-Le Reverend A. Lebkiri, C. Livera, L.D. Pettit, Inorg. Chim. Acta, 124 (1986) L19-L22.
30. V. Jószai, I. Sóvágó, Polyhedron, 30 (2011) 2114-2120.
31. C. G. Ágoston, Zs. Miskolczy, Z. Nagy, I. Sóvágó, Polyhedron, 22 (2003) 2607-2615.

Table 1. Protonation macro- and micro-constants of the ligands. I = 0.2 M (KCl), T = 298 K

Species	ADAAAC-NH_2	AADAAC-NH_2	Ac-DAAC-NH_2
$[HL]^-$	8.90(1)	8.88(1)	8.87(1)
$[H_2L]$	16.72(2)	16.67(2)	12.67(2)
$[H_3L]^+$	20.27(2)	20.38(2)	
pK_1	3.55	3.71	3.80
pK_2	7.82	7.79	8.87
pK_3	8.90	8.88	
pk_1	8.45	8.53	
pk_2	7.93	7.88	
pk_3	8.76	8.79	
pk_4	8.33	8.14	

Table 2. Stability constant of the nickel(II) complexes (log βpqr). I = 0.2 M (KCl), T = 298 K

Species	ADAAAC-NH_2	AADAAC-NH_2	Ac-DAAC-NH_2
$[NiHL]^{+}$		12.22(6)	
[NiL]	5.27(2)		3.81(9)
$[NiH_{-1}L]^{-}$	–2.96(4)	–1.78(2)	
$[NiH_{-2}L]^{2-}$	–11.03(3)	–10.62(5)	–11.78(3)
$[NiH_{-3}L]^{3-}$	–21.08(4)	–20.67(4)	–20.60(4)
$[Ni_2H_{-4}L]^{-}$		–22.80(8)	
$[Ni_2H_{-5}L]^{2-}$		–31.4(1)	

Table 3. Stability constant of the zinc(II) complexes (log βpqr). I = 0.2 M (KCl), T = 298 K

Species	ADAAAC-NH_2	AADAAC-NH_2	Ac-DAAC-NH_2
$[ZnHL]^{+}$	13.2(1)	13.3 (1)	
[ZnL]	6.37(6)	6.64(6)	5.32(6)
$[ZnH_{-1}L]^{-}$	–1.14(6)	–1.43(8)	–3.3(1)
$[ZnH_{-2}L]^{2-}$	–11.13(8)		–13.32(6)
$[ZnL_2]^{2-}$			10.34(6)

Table 4. Stability constant of the cadmium(II) complexes (log βpqr). I = 0.2 M (KNO_3), T = 298 K

Species	ADAAAC-NH_2	AADAAC-NH_2	Ac-DAAC-NH_2
$[CdHL]^+$	14.34(2)	14.86(6)	
[CdL]	7.06(2)	7.97(6)	6.51(5)
$[CdH_{-1}L]^-$	–2.07(2)	–1.99(7)	–3.2(1)
$[CdH_{-2}L]^{2-}$	–13.36(3)		
$[CdH_2L_2]$	27.87(5)	29.0(1)	
$[CdHL_2]^+$	20.34(5)	21.4(2)	
$[CdL_2]^{2-}$	11.88(3)	13.3(2)	11.9(1)
$lg(K_1/K_2)^H$	0.81	0.73	
$lg(K_1/K_2)$	2.24	2.60	1.08

Legends to Figures

Figure 1.
Concentration distribution of the species formed in the nickel(II)-AADAAC-NH_2 (A) and ADAAAC-NH_2 (B) systems ($c_{Ni(II)} = c_L = 2$ mM).

Figure 2.
Visible CD spectra of the nickel(II)-AADAAC-NH_2 system as a function of pH. The corresponding pH values are signed at the curves.

Figure 3.
CD spectra of the $[NiH_{-3}L]^{3-}$ species of AADAAC-NH_2 (a), AAAA (b), Ac-DAAC-NH_2 (c) and $[Ni_2H_{-5}L]^{2-}$ of AADAAC-NH_2 (d). Spectra (e) is calculated as the superposition of 75 % (b) and 25 % (c).

Figure 4.
Optimized structure of the energetically preferred $[NiH_{-3}L]^{3-}$ complexes of AADAAC-NH_2 (A) and ADAAAC-NH_2 at B3LYP/def2-TZVP level of theory.

Figure 5.
Concentration distribution of the species formed in the zinc(II)-AADAAC-NH_2 system ($c_{Zn(II)} = c_L = 2$ mM). The pH range of the precipitation was marked by dashed lines.

Figure 6.
Concentration distribution of the species formed in the zinc(II)-AADAAC-NH_2 (A) and AADAAH-NH_2 (B) = 1:1:1 system($c_{Zn(II)} = 2$ mM).

Figure 7.
Concentration distribution of the species formed in the cadmium(II)-AADAAC-NH_2 (A) and ADAAAC-NH_2 (B) systems ($c_{Cd(II)} = 2$ mM, $c_L = 4$ mM).

Figure 8.
Metal ions speciation of the model system containing all three metal ions and ADAAAC-NH_2 in equimolar concentrations. ($c_{Cd(II)} = c_{Zn(II)} = c_{Ni(II)} = c_L = 2$ mM)

Figure 1.

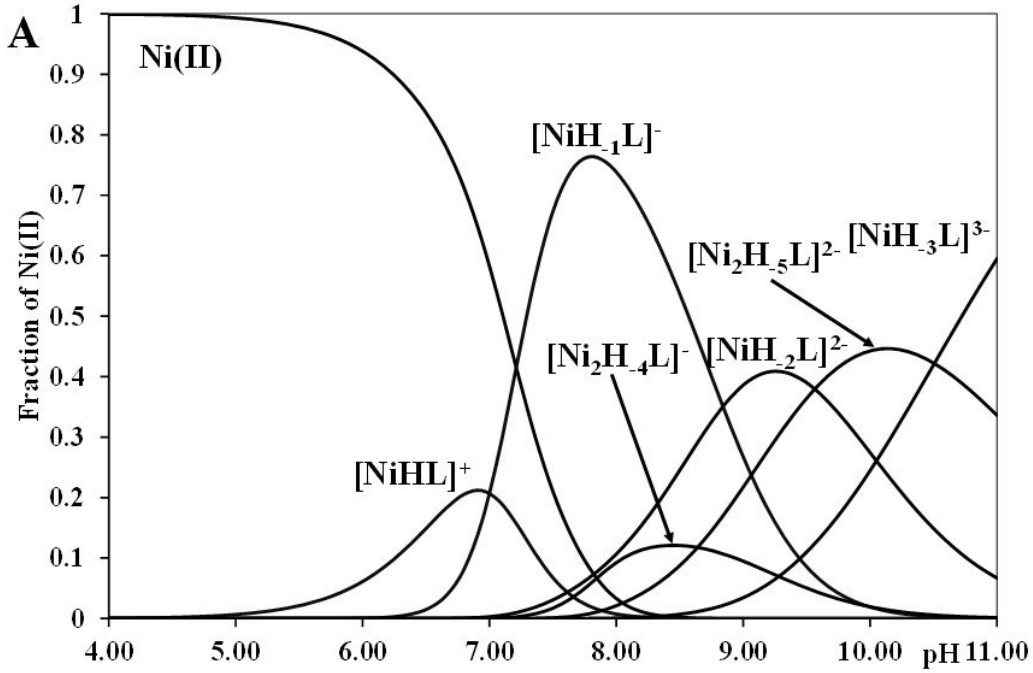

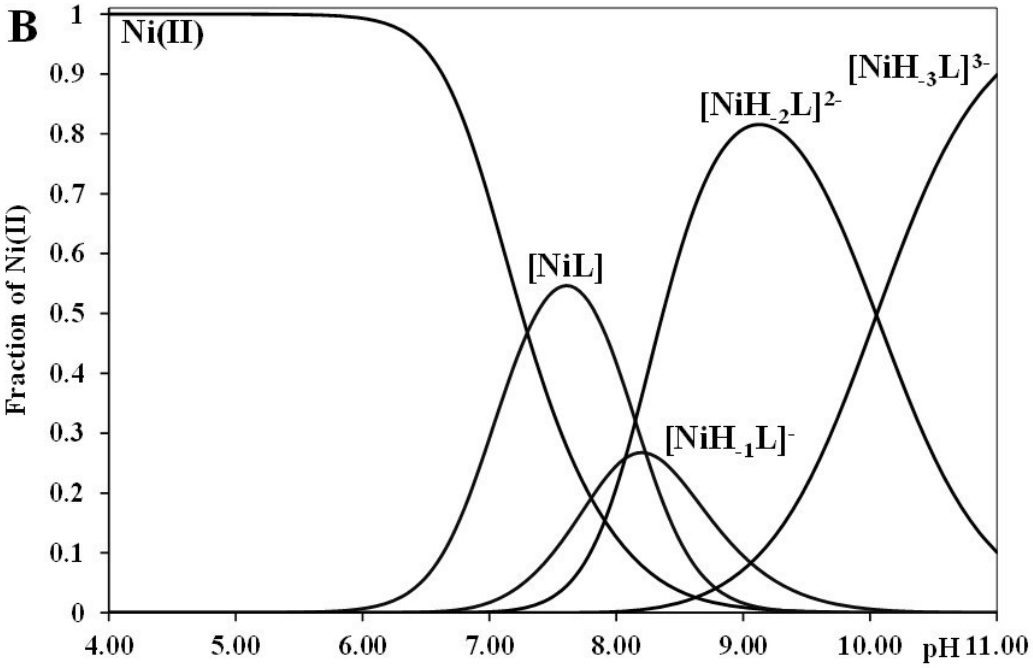

Figure 2.

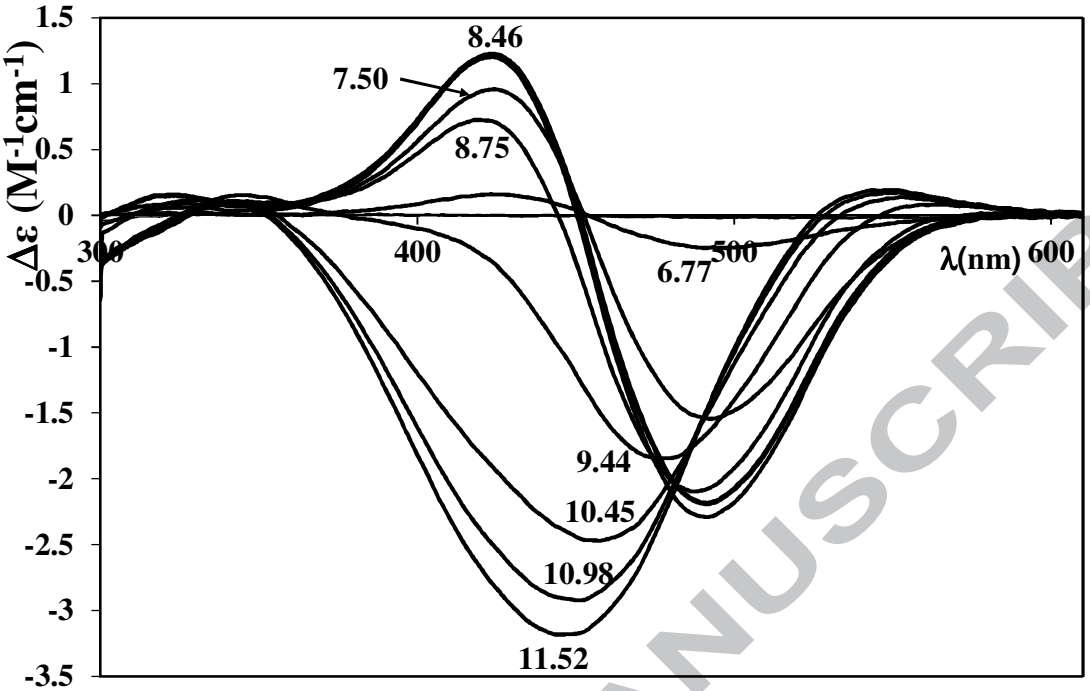

Figure 3.

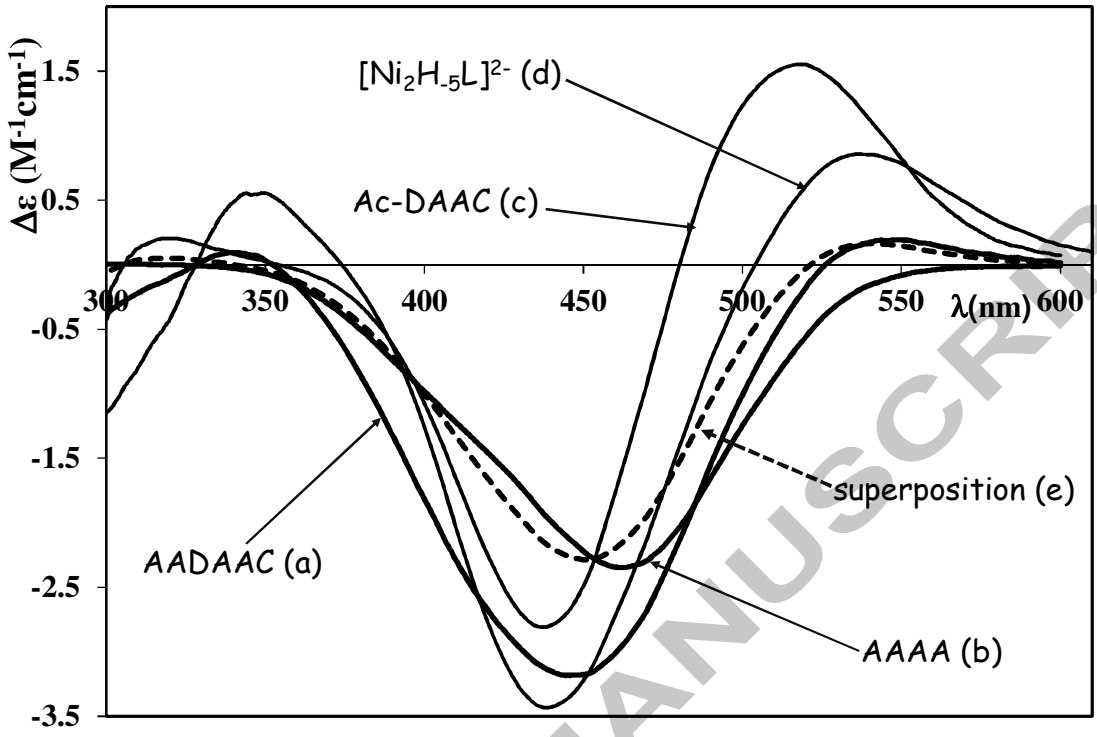

Figure 4.

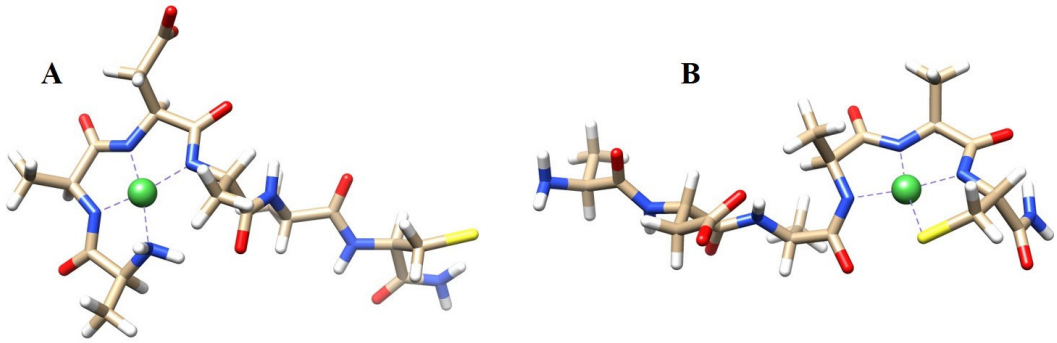

Figure 5.

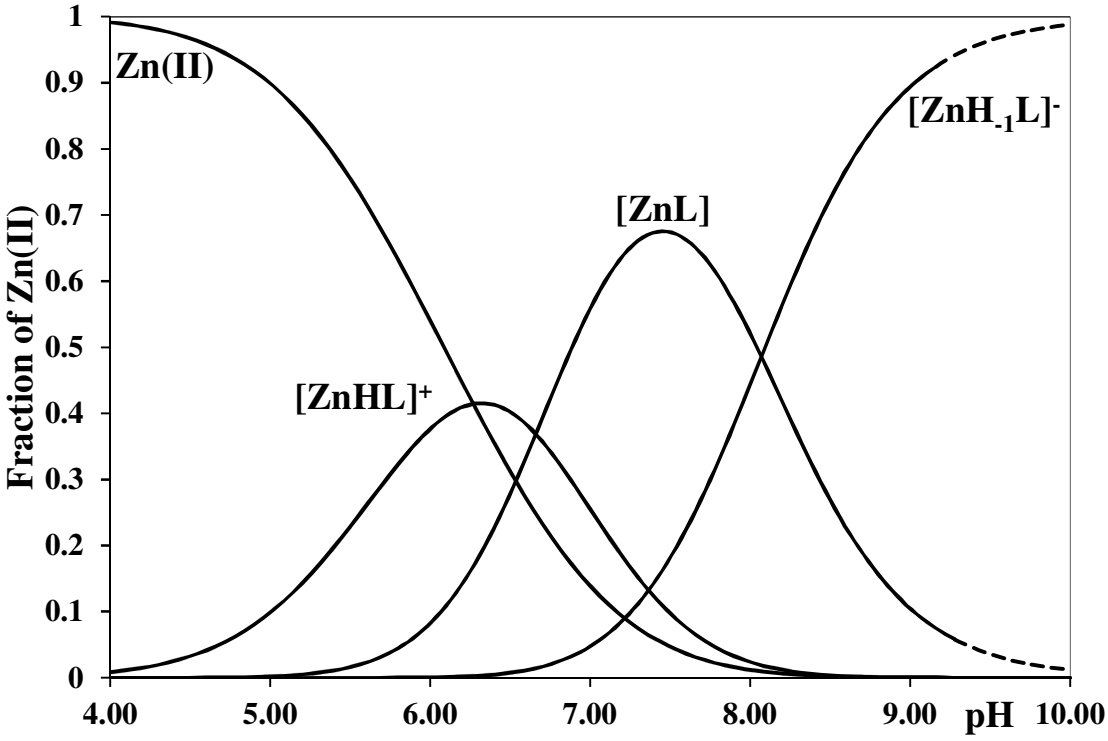

Figure 6.

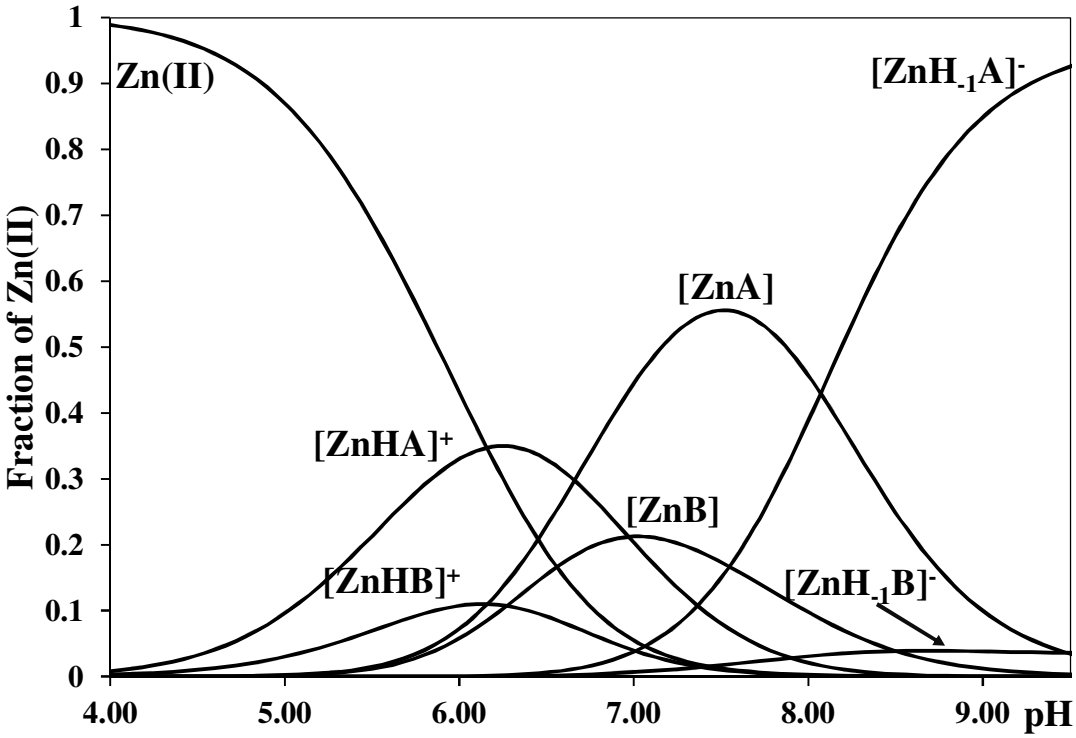

Figure 7.

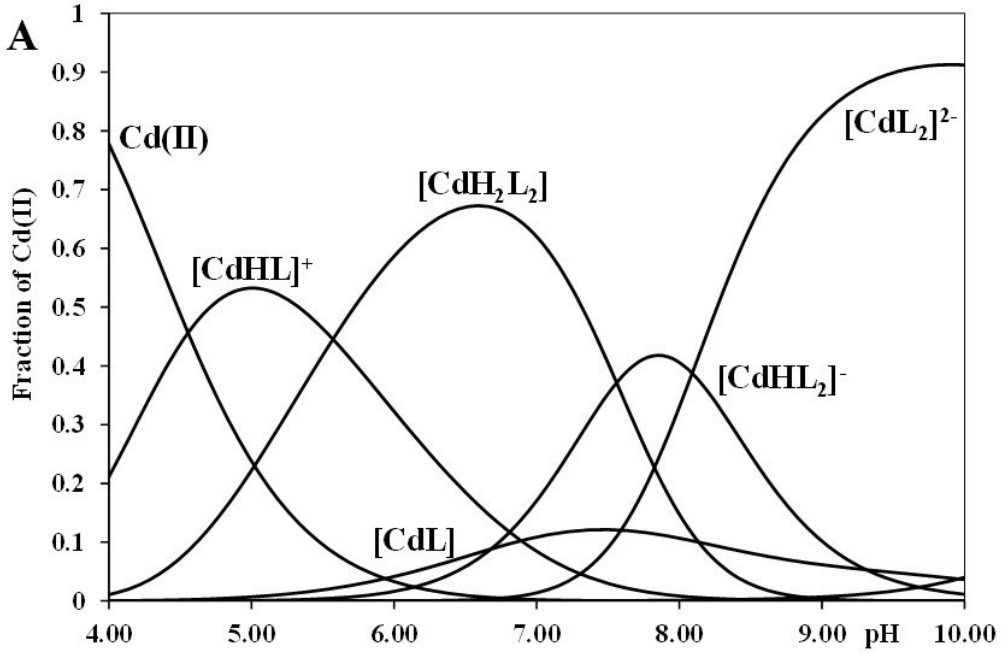

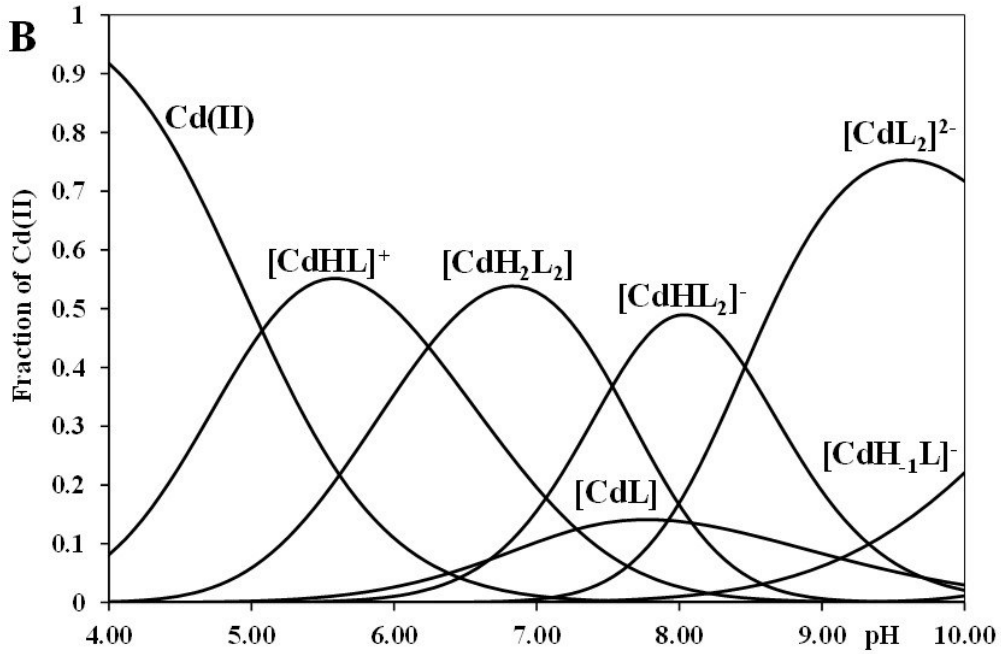

Figure 8.